

## **General Disclaimer**

### **One or more of the Following Statements may affect this Document**

- This document has been reproduced from the best copy furnished by the organizational source. It is being released in the interest of making available as much information as possible.
- This document may contain data, which exceeds the sheet parameters. It was furnished in this condition by the organizational source and is the best copy available.
- This document may contain tone-on-tone or color graphs, charts and/or pictures, which have been reproduced in black and white.
- This document is paginated as submitted by the original source.
- Portions of this document are not fully legible due to the historical nature of some of the material. However, it is the best reproduction available from the original submission.

X-616-69-398

NASA TM X-63698

# ANISOTROPIC SOLAR COSMIC RAY PROPAGATION IN AN INHOMOGENEOUS MEDIUM. II

L. F. BURLAGA

AUGUST 1969



**GODDARD SPACE FLIGHT CENTER**  
**GREENBELT, MARYLAND**

FACILITY FORM 602

~~69-39268~~

(TITLE)

(PAGES)

TMX-63698

(CODE)

29

(NASA CR OR TMX OR AD NUMBER)

(CATEGORY)

ANISOTROPIC SOLAR COSMIC RAY  
PROPAGATION IN AN  
INHOMOGENEOUS MEDIUM. II

Leonard F. Burlaga  
Laboratory for Space Sciences  
NASA-Goddard Space Flight Center  
Greenbelt, Maryland

CANNOT LOCATE  
OTHER PTS.

August 1969

## Abstract

The author's model for anisotropic solar cosmic ray propagation gives 2 coupled, partial differential equations for the intensity and anisotropy of solar cosmic rays propagating with finite speed  $V$  in an inhomogeneous medium. The model is used to study the effect of the solar shell on solar cosmic ray propagation. It predicts an exponential decay, regardless of the observer's position. It predicts that when the observer is near the center of the shell,  $t_D/t_O \approx 20$  to 30, ( $t_D$ =decay time,  $t_O$ =onset time) and  $\Lambda_m \approx 15\%$ , of  $t_m/t_O \approx 3$  to 5 ( $t_m$ =time of maximum), consistent with observations of relativistic particles on Feb. 23, 1956. When the observer is between the shell and the sun, the model predicts that oscillations might be observed near maximum intensity. When the observer moves away from the sun and the shell, the propagation is diffusive, but there is an increasingly large persistent anisotropy which serves as a measure of the width of the shell.

## I. Introduction

In a companion paper, Burlaga (1969) presented a simple, phenomenological, 1-dimensional model for anisotropic solar cosmic ray propagation. This was used to study the general effects of a diffusing region near the sun. In the present paper the mathematical model is discussed further with emphasis on the limiting results for a continuous medium, and it is applied to examine qualitatively some basic effects of the diffusing region (solar shell) which is believed to extend from somewhere near the earth to a few or several AU. (Meyer, Parker and Simpson, 1956; Parker, 1963; McCracken et al., 1967; Fan et al., 1968; Lanzerotti, 1969; Burlaga, 1967). Whereas most of the earlier work emphasized the characteristics of the total cosmic ray flux (I) measured at 1 AU, the present work examines some of the qualitative results that might be seen by detectors which measure the anisotropy and intensity of solar particle fluxes over a wide range of distances from the sun.

## II. The Model

Basic Equations. The model is as described in detail by Burlaga (1969). We consider propagation in a 1-dimensional, semi-infinite medium with a source at  $x_L=0$ . The medium is represented by an infinite number of point scattering centers which are equally spaced with separation  $\lambda$  and extend from the source to infinity. The basic equations are

$$\begin{aligned} f_{L+1, T+1}^+ &= P_L f_{L,T}^- + (1-P_L) f_{L,T}^+ \\ f_{L-1, T+1}^- &= (1-P_L) f_{L,T}^- + P_L f_{L,T}^+ \end{aligned} \quad (1)$$

where  $f_{L,T}^+$  is the probability that a particle is moving away from the source after a collision at  $L-1, T-1$  and is just approaching point  $L$  after  $T-1$  collisions,  $f_{L,T}^-$  is the corresponding probability that a particle is moving toward the source, and  $P_L$  is the probability that a particle will be reflected when it encounters a scattering center at  $x_L$ .

The Equations in the Limit of a Continuous Medium. Consider the limiting form of (1) when  $\lambda \rightarrow 0$ . Since  $\lambda = V\tau$ , where  $\tau$  is the time between successive collisions and  $V$  is the particle speed, the limit  $\lambda \rightarrow 0$  implies that  $\tau \rightarrow 0$ . In this limit we can write  $f_{L+1, T+1}^\pm \sim f^\pm(x_L + V\tau, t_T + \tau)$  which can be expanded in a Taylor's series to give

$$f_{L+1, T+1}^+ \sim f^+(x_L, t_T) + \frac{\partial f^+}{\partial x}(x_L, t_T) V\tau + \frac{\partial f^+}{\partial t}(x_L, t_T)$$

Putting this into (1), rearranging terms, and introducing the finite variable

$$D(x) \equiv \frac{\tau V^2}{2P(x)} = \frac{\lambda V}{2P(x)} \quad (2)$$

gives

$$\begin{aligned} \frac{\partial f^+}{\partial t} + V \frac{\partial f^+}{\partial x} &= \frac{V^2}{2D(x)} (f^- - f^+) \\ \frac{\partial f^-}{\partial t} - V \frac{\partial f^-}{\partial x} &= \frac{V^2}{2D(x)} (f^+ - f^-) \end{aligned} \quad (3)$$

Note that in the limit  $\tau \rightarrow 0$ ,  $P(x)$  is on the order of  $\tau$ , since  $V^2$  and  $D(x)$  remain finite. Thus, in the process of taking the limit,  $D(x)$  has replaced  $P(x)$  as the basic function characterising the inhomogeneity of the medium. Adding and subtracting (3) gives the following equations:

$$\begin{aligned} \frac{\partial I}{\partial t} + \frac{\partial J}{\partial x} &= 0 \\ J &= -D(x) \frac{\partial I}{\partial x} - \frac{D(x)}{V^2} \frac{\partial J}{\partial t} \end{aligned} \quad (4)$$

$$\text{where } I \equiv f^+ + f^- \quad (5)$$

$$\text{and } J \equiv (f^+ - f^-)V \quad (6)$$

Clearly,  $I$  is proportional to the total flux and  $J$  is proportional to the net flux. From (4) one can show that

$$\frac{\partial I}{\partial t} + \frac{D(x)}{V^2} \frac{\partial^2 I}{\partial t^2} - \frac{\partial}{\partial x} \left[ D(x) \frac{\partial I}{\partial x} \right] = \frac{1}{V^2} \frac{\partial J}{\partial t} + \frac{\partial D(x)}{\partial x} \quad (7)$$

$$\frac{\partial J}{\partial t} + \frac{D(x)}{V^2} \frac{\partial^2 J}{\partial t^2} - D(x) \frac{\partial^2 J}{\partial x^2} = 0 \quad (8)$$

In the limit  $V \rightarrow \infty$ , (7) reduces to the familiar equation for diffusion in an inhomogeneous medium. In the case  $D = \text{constant}$ , (7) and (8)

reduce to the equations that Axford (1965) derived for anisotropic propagation in a homogeneous medium. When  $D = \text{constant}$ , (3) are identical to the equations which Fisk and Axford (1969) derived from the Boltzman equation for bi-directional scattering with  $P(x) = 0.5$ . The solutions of (7) and (8) with  $D = \text{const.}$  cannot give large anisotropies except at early times, as Fisk and Axford have noted. This is because there are scattering centers everywhere which always tend to reduce the anisotropy.

Although it is customary to use solutions of the differential equations to test the theory, it is worth noting that the basic physics of the problem is contained in the expression for  $J$  in (4). It would be worth testing this directly, since it does not involve initial conditions, boundary conditions or assumptions about  $D(x)$ , and it gives a value of  $D(x)$  at the observation point which could be compared with the value computed from the power spectrum of the magnetic field.

Numerical solutions of general equations for a homogeneous medium.

Although  $P = \text{constant}$  is not very realistic for the interplanetary medium, it is worthwhile to consider solutions for this case because it is the simplest case and thus basic for an understanding of the model.

When  $P = .5$  the model reduces to the elementary random walk problem (Chandrasekhar, 1943). In this case one finds from numerical computations that

$$I = 2 \sqrt{\frac{2}{\pi T}} \exp(-L_0^2/2T) \quad (9)$$

where  $L_0$  is the number of scattering centers between the source and the observer and  $T$  is the total number of collisions that each particle has



experienced. This formula is valid only in the diffusion limit,  $L_0 \ll T$  and  $T$  large. In practice this is a remarkably good approximation, as Lord Rayleigh (1919) has noted, and valid shortly after particles first arrive at  $L_0$ . An improvement is obtained by using the solution of the telegraph equation (Axford, 1965), but for a homogeneous medium the principle difference between this solution and (9) is that the telegraph equation gives  $I=0$  when  $T < L_0$ .

When  $P < .5$  we find that an equation like (9) describes the results obtained from the model in Section II, as long as  $P$  and  $L_0$  are not too small. In particular, it is found that

$$I = 2' \frac{2}{\pi r T} e^{-\frac{L_0^2}{2rT}}, \quad T \gtrsim 1.2 L_0 \quad (10)$$

where

$$r = (1-P)/P,$$

and

$$A \equiv J/I = \frac{V}{2P} \frac{T_m}{T_0} \frac{1}{T}, \quad T \gg T_m. \quad (11)$$

Here  $T_m$  is the number of steps corresponding to the maximum of  $I$ , and  $T_0 = L_0$  is the number of steps between the source and the observer. Thus, apart from a constant multiplier, the intensity-time profile in a medium with  $P < .5$  and a given  $\lambda$  is equivalent to propagation in a medium with  $P=.5$  and  $\lambda' = r\lambda$ . Axford (private communication) has pointed out that a similar result was obtained analytically by Goldstein (1951) for  $P=\text{constant}$ .

To transform the above results to dimensional form, let  $x \equiv L\lambda$ ,  $t \equiv T\tau$ , and

$$D = \frac{r\lambda V}{2} \quad (12)$$

Then

$$N \equiv \frac{I}{\lambda} = \sqrt{\frac{2}{\pi D t}} e^{-\frac{x_0^2}{4Dt}} \quad (13)$$

and

$$A = \frac{D t_m}{Pr V x_0} \frac{1}{t} \quad (14)$$

In the diffusion limit  $\lambda \rightarrow 0$ ,  $v \rightarrow \infty$ ,  $P \rightarrow 0$ , and  $Pr \rightarrow 1$ ; thus, with the relation  $t_m = x_0^2 / (2D)$ , one obtains

$$A = \frac{x_0}{2Vt} = -\frac{D}{N} \frac{\partial N}{\partial x} \quad (15)$$

Equations (13) and (15) are the usual results for diffusion in 1-dimension.

### III. Solar Shell

The solar shell is the cosmic ray diffusion region in the vicinity of the earth. A thorough mathematical study of the shell requires a knowledge of  $P(x)$ , inclusion of the effects of the solar envelope, and consideration of both parallel and transverse diffusion (Burlaga, 1967, Bukata et al., 1969). Such an investigation involves several parameters which are not known experimentally, so a parameter study at this time is neither practical nor illuminating. Our approach will therefore be to study an idealized model which contains what we consider to be essential features of the real situation. The aim is to obtain a qualitative understanding of the effects of a shell which might be observed by spacecraft near and far removed from the earth's orbit. When more measurements are available, particularly measurements concerning  $P(x)$  (actually  $D(x)$ ) which can be obtained by deep space probes, it will be meaningful to apply the model to fit actual observations in detail.

We consider one-dimensional propagation as described in Section II. This will be a reasonable approximation if the flare is near a magnetic field line which passes through the observation point. Recent calculations of the diffusion constant based on magnetic field observations suggest that diffusion is essentially 1-dimensional near 1 AU, (contrary to the assumption of Burlaga (1967)), but transverse diffusion may still occur in the envelope and give rise to East-West effects in essentially the same way as calculated by Burlaga). It is well known that the effect of additional degrees of freedom in diffusive propagation is manifested by a power-law dependence in time. For example, the Green's function for 1-dimensional diffusion is

proportional to  $t^{-1/2} \exp(-x^2/4Dt)$  while for 3-dimensional diffusion it is proportional to  $t^{-3/2} \exp(-x^2/4Dt)$ . Thus, the important qualitative features of the propagation will not be lost by considering 1-dimensional propagation.

As in previous work (Burlaga 1967, 1969), we shall assume an instantaneous point source and a non-absorbing boundary at the sun. We shall assume that the sun's surface reflects particles, but replacing the sun by interplanetary scattering centers would not qualitatively change the intensity-time profiles. To avoid specifying parameters characterizing the solar envelope, we shall neglect the envelope altogether. Now, it is known that the envelope tends to store particles and thus acts as a modified source (Burlaga, 1969; Shishov, 1966). For the  $>1$  bv particles on May 4, 1960 the characteristic "injection time" for this source was  $t_i \sim 15$  min. For the much lower energy particles on March 24, 1966, the same type of analysis gives an injection time  $t_i \sim 60$  min. When the characteristic times of the observed intensity-time profiles are much greater than  $t_i$ , one can assume an instantaneous source with little error. When the characteristic times approach  $t_i$  the "smoothing" effects of the envelope will be seen, and when the characteristic times are  $\geq t_i$ , the approximation is invalid.

The geometry of the solar shell is poorly understood. At times there seems to be little scattering between the solar envelope and the earth (McCracken et al, 1967; McCracken, 1962) and in general the diffusion seems to cease beyond  $\sim 2$  AU (Burlaga 1967). As a zeroth approximation to  $P(x)$  we shall take  $C \exp(-(L-L_s)/L_w)^2$ . The assumption of symmetry is introduced solely for simplicity and has no basis in

observational facts. This is a point which must be examined by deep-space probes. The shell is centered at  $L_s$  and contains  $\sim 2L_w$  effective scattering centers. The characteristic diffusing length is determined by putting the observer at  $L_o$ . (Note that  $L_o$  is now independent of the solar envelope). For simplicity, we set  $C=.5$ . Equivalent qualitative results could be obtained for smaller  $C$  by increasing  $L_o$  and  $L_w$ , but the case  $C=.5$  will serve to reveal the basic features of the propagation.

With the above approximations, the model is rather simple. The results will now be discussed for three different cases:  $L_s \sim L_o$ ,  $L_s < L_o$ , and  $L_s > L_o$ .

$L_o = L_s$ . First consider  $L_o = L_s$ , corresponding to an observer in the middle of the shell. A typical intensity-time profile is shown in Figure 1, which gives the solution for  $L_o=20$ ,  $L_s=20$  and  $L_w=10$ . The sunward flux rises gradually, reaches a maximum at  $T_m$ , and then decays exponentially with an e-folding time  $T_D$ . The anti-sun flux does the same, with the same  $T_D$  but a larger  $T_m$ . The results can be summarized by the parameters  $T_m/T_o$ ,  $T_D/T_o$ ,  $A_m$  and  $A_\infty$ , where  $T_o$  is the onset "time" (the number of steps required to reach  $L_o$ ),  $A_m$  is the anisotropy at the time of maximum intensity of the total flux, and  $A_\infty$  is the anisotropy at very large  $T$ . Here anisotropy is defined by the equation

$$A \equiv \frac{f^+ - f^-}{f^+ + f^-}.$$

Several models were examined, with  $L_o=10, 20, 40$ , and  $L_w$  ranging from 3.33 to 40. It was found that the parameters describing the intensity-time profiles are determined primarily by  $L_w$ . Figure 2 shows

$T_m/T_o$ ,  $T_D/T_o$ , and  $A_m^{-1}$  versus  $L_w$  for the various cases. Note

the linear relationships. Also note that  $L_w$  determines each of the 3 observable quantities. Conversely, measuring these 3 quantities provides a strong test of the applicability of the model since they must all be related as required by the inferred  $L_w$ . For example,  $T_D/T_O = 15$  implies that  $L_w = 10$  which in turn implies that  $T_m/T_O = 5.5$ , and  $A_m \approx 30\%$ .

When the shell is very thin ( $L_w \leq 5$ ) the profile is similar to that in Figure 1, except that there is a "precursor". This is caused by the relatively large number of particles which arrive at  $T_O$  without scattering because of the small  $L_w$ .

Observations of relativistic solar particles on Feb. 23, 1956, reported by Meyer et al. (1956), show an intensity-time profile which is similar to those in Figure 1 and a rapid approach to anisotropy as implied by the model for  $L_O = L_s$ . Furthermore the flare was near the base of the field line passing through the earth (Burlaga, 1967), and the smallest characteristic time,  $t_m \sim 130$  min, was much larger than the time of escape from the envelope (15 min) for similar particles on May 4, 1960, so one might expect the above model to apply. Table 1 shows  $t_m/t_O$  and  $t_D/t_O$  for particles monitored at Ottawa ( $\geq 1$  bv), Chicago ( $\geq 1.9$  bv) and Wellington ( $\geq 3.4$  bv). The values of  $t_m$  and  $t_D$  are from Webber (1964) and the values of  $t_O$  are rectilinear propagation times to earth for protons of the indicated rigidities. For the given  $t_m/t_O$  one can find the  $L_w$  from Figure 2 and then a predicted  $t_D/t_O$ , and  $A_m$ . Table 1 shows that the observed and predicted values of  $t_D/t_O$  are in reasonable agreement. (Exact agreement would be coincidental because of the assumptions in the model). The quantity

$A_m$  was not measured directly, but the values shown in Table 1 are consistent with the observed rapid approach to near isotropy (Meyer et al. 1956, Lüst and Simpson, 1957). Thus, the observations suggest that the middle of the solar shell was near the earth on Feb. 23, 1956.

$$\underline{L_o < L_s.}$$

Now consider the case of an observer who is between the sun and the center of the shell. Figure 3 shows  $f^+$ ,  $f^-$ , and  $A$  versus  $T$  for  $L_w=20$  and  $L_s=30$ . This illustrates the general case which shows a strong beam of particles arriving at  $T_o$  and moving toward the scattering region. Particles are reflected from the shell and move toward the sun where they are again reflected. The process continues so that one observes a damped train of oscillations in  $f^+$  and  $f^-$  which are out of phase such that the anisotropy also fluctuates. At late times the decay is exponential and the anisotropy tends to zero. The decay time is much larger than in the case  $L_o=L_s$ , and it depends appreciably on  $L_s$  as well as  $L_w$ . This is shown in Table 2.

The 'period' of the oscillations is essentially constant. It equals  $2(L_s - L_w)$  when  $L_w < 20$  and is somewhat smaller for larger  $L_w$ . The damping is simply the result of diffusion. Thus a thicker shell gives smaller amplitude oscillations and the amplitude of the oscillations is smaller when the observer is closer to the center of the shell. As one would expect, the oscillations are found to be very small when  $L_o \sim L_w$ ; in this case the shell extends to the sun and particles diffuse everywhere.

In order to observe these oscillations their period, which is approximately twice the time required for a particle to move from the sun to the shell, must be larger than the time for particles to escape from the envelope. If the shell center were at  $\sim 2$  AU the period would be  $\sim 45$  min. for 1 bv particles so one might expect to see the oscillations at the earth. Even if the shell were centered at  $\sim 1$  AU, the period would be  $\sim 12$  min. which is probably comparable to the ejection time for the envelope, and weak oscillations might be seen by instruments moving close to the sun. The real beam is not mono-energetic, as assumed in the model, and there will be complications arising from pitch angle scattering, mirroring, patches of turbulence, etc. All of these effects tend to damp the oscillations, so one cannot say from our model that the oscillations will be seen, only that they might be seen. If they are seen they can be used to probe the shell.

Oscillations in solar cosmic ray fluxes have been observed (see the review by Williams, 1969), but they are usually non-dispersive or have the 'wrong' period. (It is conceivable that the period could be velocity independent if the characteristics of the shell were appropriately velocity dependent, but this would require a special coincidence.) McCracken (1962) has reported particularly interesting observations of relativistic particles on Nov. 12, 1960 from several stations which view in various directions. Fluctuations in intensity, which could be interpreted as oscillations with a period  $\sim 20$  min were observed at 2 stations which looked toward the sun, but the anti-sun flux does not show oscillations with the proper phase. The very large anisotropies for the first 30 min. suggest that particles were stored for nearly this time in the envelope, which would also argue against



the detection of 20 min. oscillations. Thus, there is as yet no convincing evidence for the oscillations predicted by the model. However, the shell is probably near the earth and, as noted above, this situation is not ideal for detecting the oscillations. They are more likely to be seen by instruments at  $\sim 0.5$  AU. Relatively long decay times are likely to be observed at such distances even if the oscillations are not seen.

$$\underline{L_O > L_S.}$$

Finally, consider an observer who is beyond the center of the shell. Models with  $L_O = L_S + L_W$ , where  $L_O = 10, 20, 40$  and  $L_W = L_O/2$  show that  $f^+$  and  $f^-$  rise gradually to a maximum and then decline exponentially. A typical profile is shown in Figure 4. Figure 5 shows that the ratio  $T_m/T_O$  varies linearly with  $L_W$  in essentially the same way as shown in Figure 2 for  $L_O = L_W$ . However, the decay time is much larger when  $L_O = L_S + L_O/2$  than when  $L_O = L_S$ , and it depends on  $L_S$  as well as  $L_W$ . The anisotropy is large, ranging from 30% when  $L_W = 20$  to 80% when  $L_W = 3.3$ , and  $A_\infty \approx A_m$ . Figure 5 shows that  $A$  varies linearly with  $L_W$ . When  $L_O = L_S + aL_W$  where  $a > 1$ , the anisotropy increases because there is less backscattering beyond the observer.

The observations at 1 AU never show a large anisotropy at late times, although small anisotropies have been observed (McCracken et al. 1967), and attributed to effects other than geometry. However, when instruments are carried toward the outer planets, large anisotropies at late times and large decay times should be observed. Clearly, measurements of the anisotropy would provide a means of determining the relative position of the shell and are thus highly recommended.

#### ACKNOWLEDGEMENTS

The author thanks Drs. N. F. Ness, K. W. Ogilvie, and K. Schatten for critically examining the manuscript. The programming was done by Mr. Thurston Carlton.

TABLE 1. Parameters for the February 23, 1956, Event

	$t_m/t_o$	$L_w$	$t_D/t_o$	$t_D/t_o(th.)$	$A_m(th.)$
1 bv	5.2	10.5	21	27	~15%
1.9 bv	4.4	9.3	21	24	15%
3.4 bv	3.8	8.5	15	22	15%

TABLE 2. Decay 'time' versus  $L_w$  and  $L_s$  for  $L_s < L_o$

$L_w$	$L_s$	$T_D$
3.33	13.33	130
	16.33	165
	20	200
5	20	210
	30	285
	40	260
10	30	805
	40	1095
	50	1390
20	40	2020
	60	3140
	80	4280
	100	4635
40	80	5680
	120	7785
	160	9200

FIGURE CAPTIONS

Figure 1. 'Intensity-time' profiles for 'sunward' (+) and 'anti-sun' (-)'fluxes' for an observer at the center of a shell whose thickness is comparable to the distance between its center and the source. Specifically,  $f(L,T)$  is the probability of finding a particle at the  $L^{\text{th}}$  scattering center from the source after it has made  $T$  collisions. Note the gradual rise to maximum, the exponential decay, and the small persistent anisotropy at late times. The anisotropy is shown at the bottom of the figure.

Figure 2. For events with  $L_0=L_w$ , such as that in Figure 1,  $T_m/T_0$ ,  $T_D/T_0$  and  $A_m^{-1}$  are determined primarily by  $L_w$  and vary with  $L_w$  as shown here. The subscripts m, D and zero refer to the times of maximum, decay, and onset, respectively.

Figure 3. When the observer is between the shell and the source, the model predicts oscillations in the fluxes and anisotropy, as illustrated here. Note that the shell has the same thickness and the observer is at the same position as the case in Figure 1, but the shell is farther removed from the source.

Figure 4. When the observer is beyond the shell, the 'intensity-time' profiles are 'diffusive', but a large anisotropy is predicted during the decay because there is little

backscattering beyond the shell.

Figure 5. When the observer is beyond the shell,  $T_m/T_o$  and the anisotropy at maximum intensity and during the decay are linearly related to  $L_w$  as shown here.

REFERENCES

- Axford, W. I., 1965, Planet. Space Sci., 13, 1301.
- Bukata, R. P., Gronstal, P. T., Palmeira, E. A. R., McCracken, K. G.,  
and Rao, U. R., 1969, to appear in Solar Physics.
- Burlaga, L. F., 1967, J. Geophys. Res., 72, 4449.
- Burlaga, L. F., 1969, NASA-GSFC Preprint X-616-69-281, to appear in the  
Proceedings of the Eleventh International Conference on Cosmic Rays.
- Chandrasekhar, S., 1943, Rev. Mod. Phys. 15, 1.
- Fisk, L. A., and Axford, W. I., 1969, Solar Physics (to appear).
- Goldstein, S., 1951, Quart. J. Mech. Appl. Math., 4, 129.
- Lanzerotti, L. J., 1969, J. Geophys. Res., 74, 2851.
- Lust, R., and Simpson, J. A., 1957, Phys. Rev., 108, 1563.
- McCracken, K. G., 1962, J. Geophys. Res., 447.
- McCracken, K. G., Rao, U. R., and Bukata, R. P., 1967, J. Geophys.  
Res., 72, 4293.
- Meyer, P., Parker, E. N., and Simpson, J. A., 1956, Phys. Rev. 104, 768.
- Parker, E. N., 1963, Interplanetary Dynamical Processes (New York:  
Interscience)
- Rayleigh, 1919, Phil. Mag., 37, 321.
- Shishov, V. I., 1966, Geomagn. i aeronomiya 4, 223.
- Webber, W. R., 1964, in AAS-NASA Symposium on the Physics of Solar  
Flares, NASA SP-50, ed. by W. N. Hess.
- Williams, D. J., 1969, NASA-GSFC X-612-69-258.

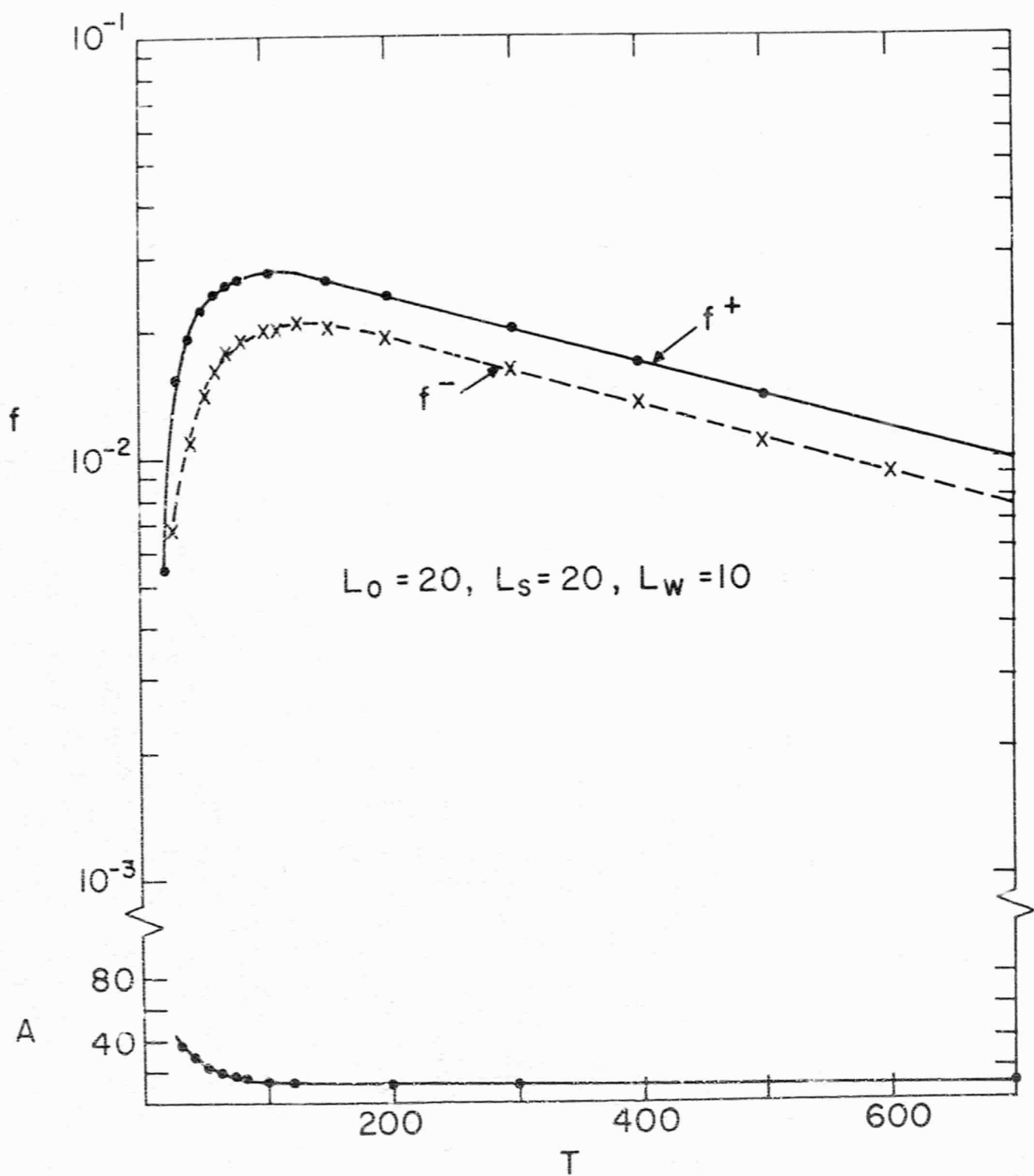


Figure 1



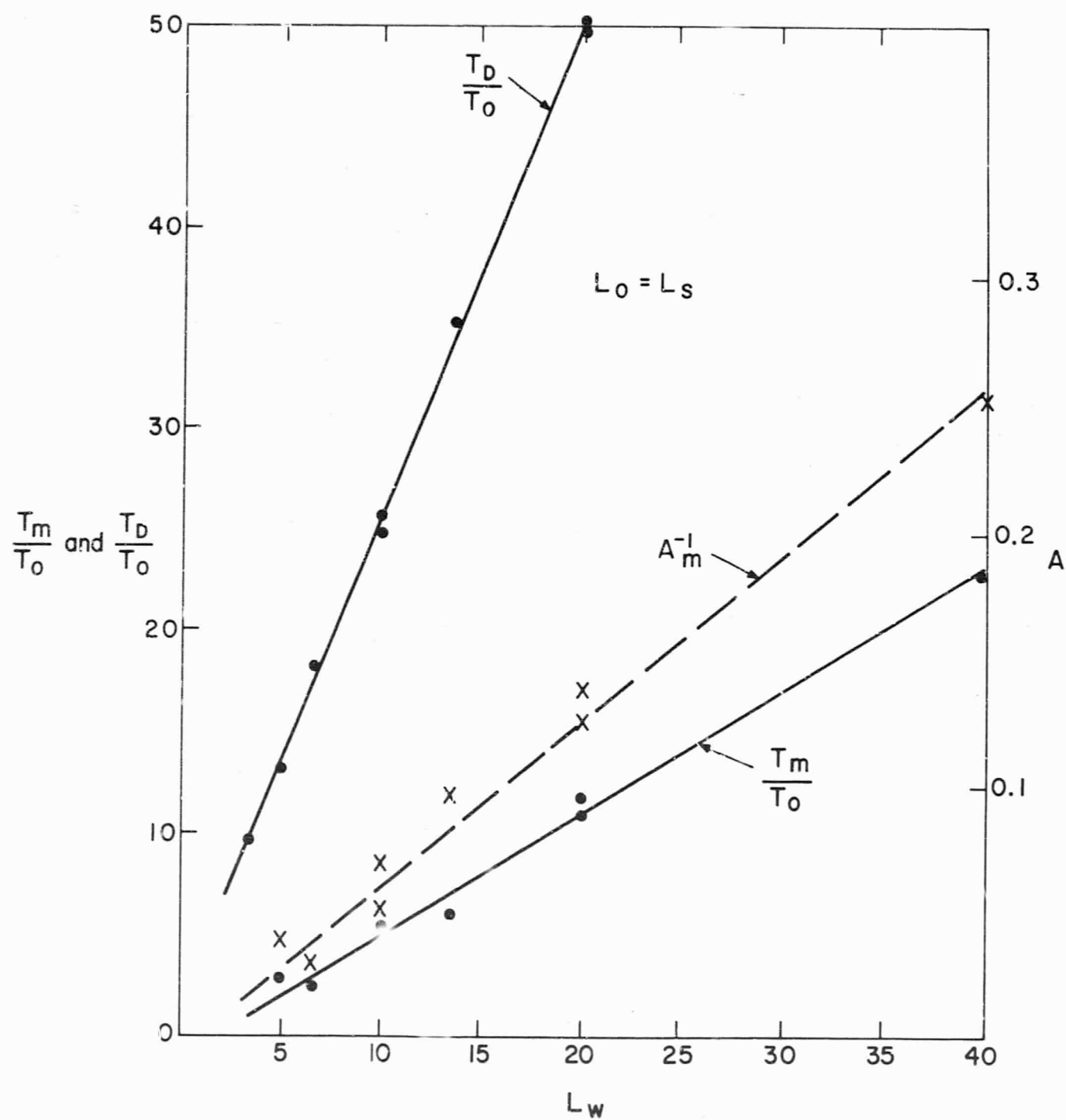


Figure 2

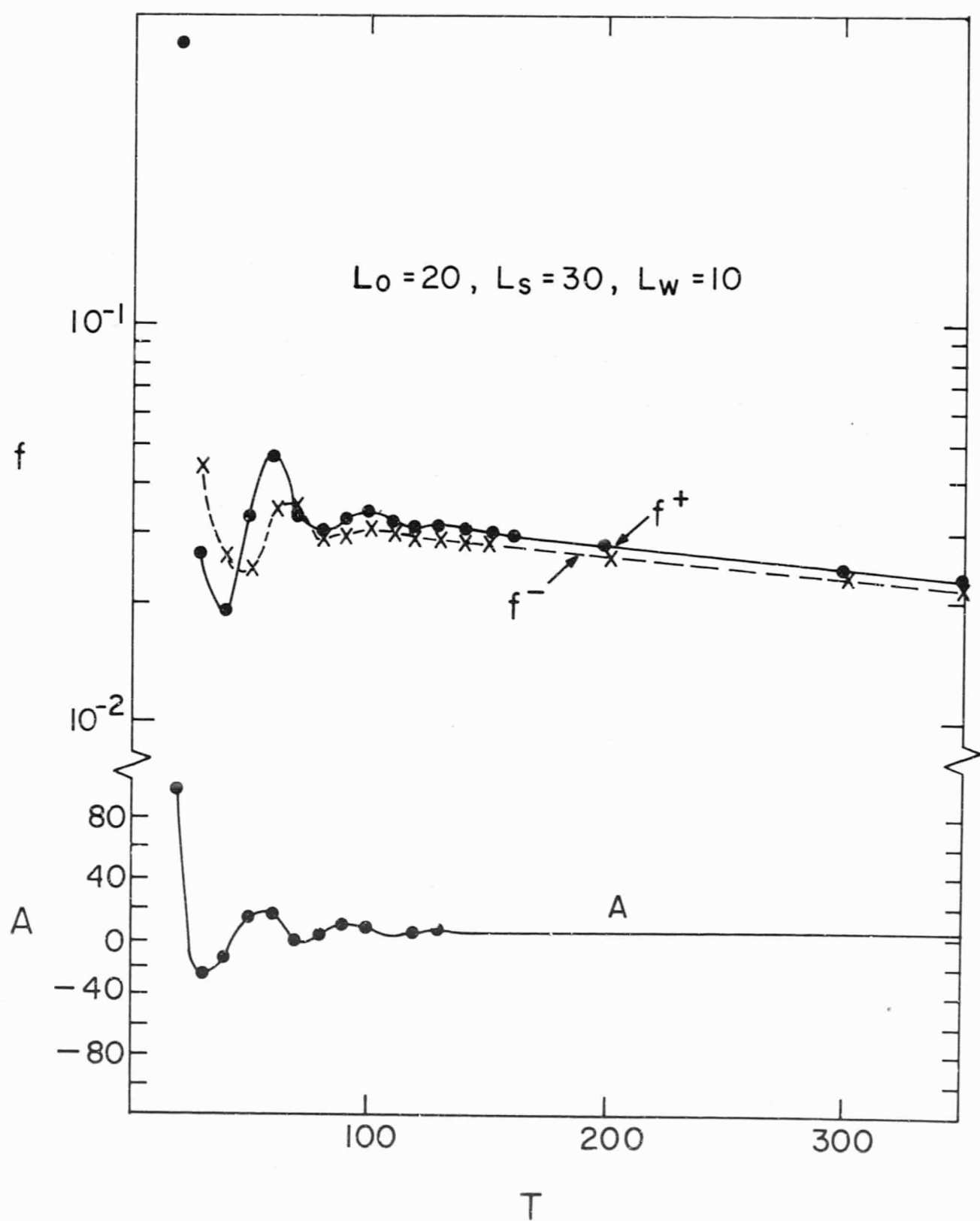


Figure 3

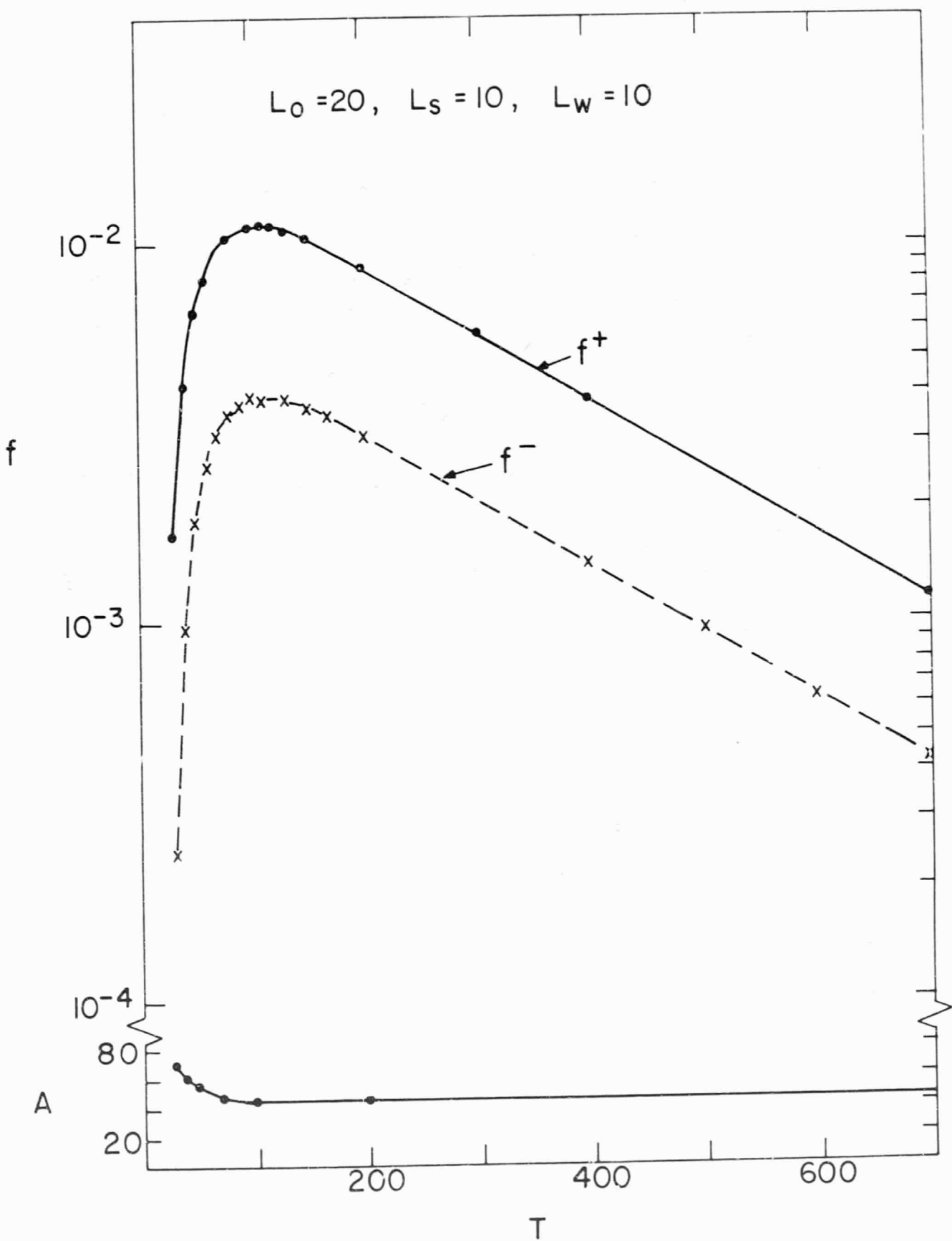


Figure 4

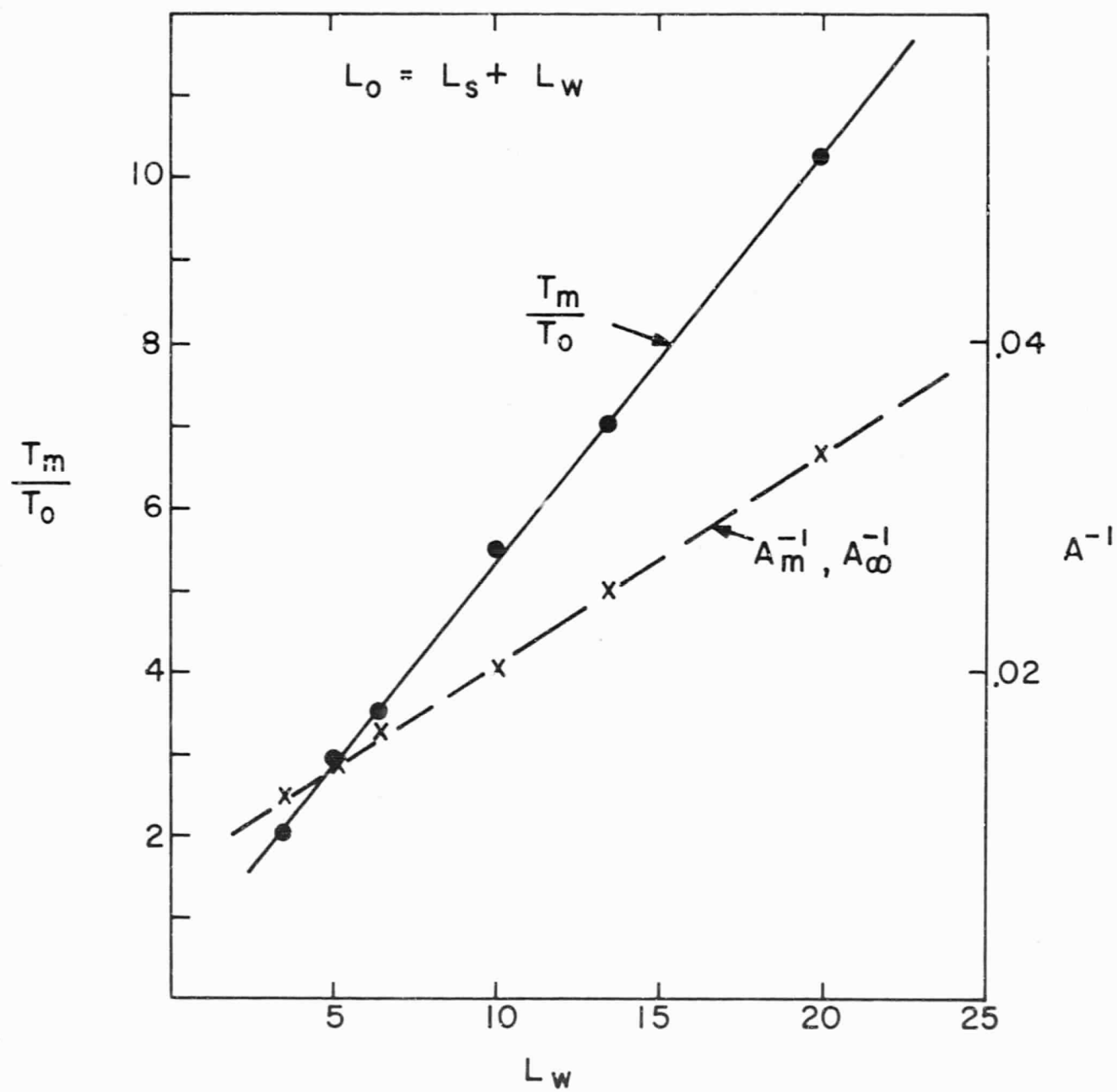


Figure 5